Advances in Fatigue Lifetime Predictive Techniques

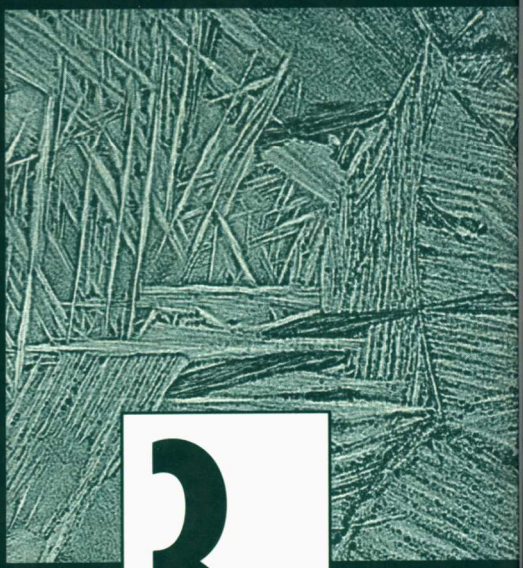

3rd volume

M. R. MITCHELL
R. W. LANDGRAF
editors

ASTM STP 1292

STP 1292

Advances in Fatigue Lifetime Predictive Techniques: 3rd Volume

M. R. Mitchell and R. W. Landgraf, editors

ASTM Publication Code Number (PCN):
04-012920-30

ASTM
100 Barr Harbor Drive
West Conshohocken, PA 19428-2959

Printed in the U.S.A.

Library of Congress Cataloging-in-Publication Data

ISSN: 1070-1079
ASTM Publication Code Number (PCN): 04-012920-30
ISBN: 0-8031-2029-X

Peer Review Policy

Each paper published in this volume was evaluated by three peer reviewers. The authors addressed all of the reviewers' comments to the satisfaction of both the technical editor(s) and the ASTM Committee on Publications.

The quality of the papers in this publication reflects not only the obvious efforts of the authors and the technical editor(s), but also the work of these peer reviewers. The ASTM Committee on Publications acknowledges with appreciation their dedication and contribution to time and effort on behalf of ASTM.

Printed in Ann Arbor, MI
January 1996

Foreword

This publication, *Advances in Fatigue Lifetime Predictive Techniques: 3rd Volume,* contains papers presented at the Third Symposium on Advances in Fatigue Lifetime Predictive Techniques, which was held in Montreal, Quebec on 16–17 May 1994. The symposium was sponsored by ASTM Committee E-08 on Fatigue and Fracture and by Subcommittee E08.05 on Cyclic Deformation and Fatigue Crack Formation. Symposium co-chairmen were M. R. Mitchell, Rockwell Science Center, Thousand Oaks, CA, and R. W. Landgraf, Virginia Polytechnic Institute and State University, Blacksburg, VA.

Overview

This volume, the third in a series on fatigue lifetime predictive techniques [see *ASTM STP 1122* (1991) and *STP 1211* (1993)], continues the tradition of providing a cross-disciplinary forum bringing together researchers and practitioners representing industry, universities, and government for the purpose of sharing knowledge and experiences associated with the important technological issue of understanding and controlling fatigue failures in components and structures. With the continuing trends toward structural weight reduction, performance optimization, and the application of tailored materials and structural elements, fatigue analysis has become an integral part of engineering design. Indeed, the availability of reliable life prediction methods can prove invaluable in developing durable products more quickly and at lower cost—issues of considerable concern for achieving global competitiveness.

As in past volumes, topical coverage among the 17 papers is broad and includes treatment of fundamental fatigue mechanisms as well as the development and application of fatigue design and analysis strategies. Composite materials continue to command the attention of researchers. The first two papers deal with the complexities of metal matrix composites exposed to combined mechanical and thermal environments. Neu and Nicholas present two analysis methods that account for multiple failure mechanisms as influenced by frequency, temperature, phasing, and environmental kinetics. Tamin and Ghonem discuss a combined analytical-experimental approach for studying cyclic and creep loading with emphasis on strain compatibility and the development and stability of thermal residual stresses.

The paper by Strait et al. explores thermo-mechanical fatigue in polymer matrix composites demonstrating the significant effect of level of constraint on system response and damage development. Elastomer composites are the subject of the paper by Liu and Lee in which a variety of nondestructive methods for detecting damage are evaluated.

Damage mechanics is another active area of research. Two papers deal with general computational fracture mechanics methods for life prediction. Chow and Wei extend a two-damage surface model in conjunction with finite element analysis to predict crack propagation in aluminum plates. Energy concepts are employed by Chang et al. to develop a general method for predicting crack initiation and growth using only uniaxial tensile data.

Crack initiation and growth at notches is the subject of papers by Hou and Lawrence, and Prakash et al. The first treatment involves a plasticity modified strip-yield model to account for the observed crack growth retardation following an overload. The second paper, employing fractographic and replication techniques to chart cracking behavior under spectrum loading, presents a growth model allowing for interaction of multiple cracks. In an experimental investigation of crack growth from a surface flaw under biaxial stress cycling, Zamrik and Ryan quantify the effect of biaxial ratio and a transition from Mode I to Mode II crack growth.

Microstructural effects on fatigue cracking behavior is the subject of the next two papers. Hardy investigates short crack behavior in a near α-titanium with emphasis on the early, microstructure-dependent behavior for which LEFM is not applicable and presents a two-stage empirical model that includes crack opening loads and identifies critical crack sizes above which fracture mechanics techniques do apply. Evans et al. likewise deal with a titanium alloy in developing a comprehensive database approach to component life estima-

tion that considers microstructural interactions and local plasticity in establishing an initial flaw size for calculations.

The final set of papers highlight the development and application of design methods for dealing with fatigue in components and structures. Bunch et al. detail the fatigue analysis methods used during the design and development of the B-2 bomber, while Sundar and Prakash consider lug joint performance under spectrum loading. Sheppard presents a continuation of her work on spot weld fatigue, extending the range of applicability to a variety of specimen types and notch profiles, including those subjected to post-weld treatments, and to the development of guidelines for selective thickening. Fatigue of coiled tubing, as used in oil drilling, is the subject of Tipton's paper in which he develops a damage parameter based on multiaxial plasticity analysis to predict combined pressurization and coiling events.

Reliability methods are employed by Kliman et al. to compute fatigue life distribution functions under time-varying loading sequences. Finally, the paper by Kalluri et al. addresses the often important influence of prestraining of components, as a result of manufacturing or service overstrains, on damage accumulation.

Taken as a whole, the papers in this volume provide ample evidence that important progress continues in our efforts to better understand and, hence, to control fatigue failure in a range of engineering structures. There is a clear trend among researchers toward confronting the many complexities of "real world" material systems, structural configurations, and service environments in arriving at more powerful tools for fatigue design and analysis. Further, the transfer of this new technology to engineering practice, long a challenge, appears to be proceeding in a timely manner. It is the derived practical benefits from past research efforts that provide an important impetus for further studies.

Michael R. Mitchell
Rockwell Science Center
Thousand Oaks, CA 91360
Symposium co-chairman and co-editor

Ronald W. Landgraf
Virginia Polytechnic Institute & State University
Blacksburg, VA 24061
Symposium co-chairman and co-editor

Contents

Richard W. Neu[1] *and Theodore Nicholas*[2]

Methodologies for Predicting the Thermomechanical Fatigue Life of Unidirectional Metal Matrix Composites

REFERENCE: Neu, R. W. and Nicholas, T., **"Methodologies for Predicting the Thermomechanical Fatigue Life of Unidirectional Metal Matrix Composites,"** *Advances in Fatigue Lifetime Predictive Techniques: 3rd Volume, ASTM STP 1292*, M. R. Mitchell and R. W. Landgraf, Eds., American Society for Testing and Materials, 1996, pp. 1–23.

ABSTRACT: Parameters and models to correlate the cycles to failure of a unidirectional metal matrix composite (SCS-6/Timetal 21S) undergoing thermal and mechanical loading are examined. Three different cycle types are considered: out-of-phase thermomechanical fatigue (TMF), in-phase TMF, and isothermal fatigue. A single parameter based on either the fiber or matrix behavior is shown not to correlate the cycles to failure of all the data. Two prediction methods are presented that assume that life may be dependent on at least two fatigue damage mechanisms and therefore consist of two terms. The first method, the linear life fraction model, shows that by using the response of the constituents, the life of these different cycle types are better correlated using two simple empirical relationships: one describing the fatigue damage in the matrix and the other fiber-dominated damage. The second method, the dominant damage model, is more complex but additionally brings in the effect of the environment. This latter method improves the predictions of the effects of the maximum temperature, temperature range, and frequency, especially under out-of-phase TMF and isothermal fatigue. The steady-state response of the constituents is determined using a 1-D micromechanics model with viscoplasticity. The residual stresses due to the CTE mismatch between the fiber and matrix during processing are included in the analysis.

KEYWORDS: metal matrix composites, titanium matrix, silicon carbide fibers, thermomechanical, fatigue, elevated temperature, micromechanics

One of the challenges of advanced metal matrix composites (MMCs) involves developing life prediction methodologies since most applications for these composites involve complex stress-temperature-time histories. The coefficient of thermal expansion (CTE) mismatch between the fiber and matrix and resulting thermal residual stresses from processing further add to the complexity. In general, a model that is capable of predicting life under different cycles and test conditions is desired. To simplify the present problem, three basic cycle types are identified: isothermal fatigue (IF), out-of-phase (OP) TMF, and in-phase (IP) TMF. The waveforms are triangular, and in OP TMF, the maximum stress and minimum temperature coincide, while in IP TMF, the maximum stress and maximum temperature coincide. The methodologies are evaluated under different test conditions, which include changes in the maximum temperature (T_{max}), temperature range (ΔT), and frequency. The aim of this investigation is to identify methodologies that are successful in correlating and predicting all three different cycle types under the various test conditions.

[1]Formerly, NRC associate, Wright Laboratory Materials Directorate, Wright-Patterson AFB, OH 45433-7817; currently, assistant professor, George W. Woodruft School of Mechanical Engineering, Georgia Institute of Technology; Atlanta, Ga 30332-0405.

[2]Senior scientist, Wright Laboratory Materials Directorate, Wright-Patterson AFB, OH 45433-7817.

Examination of the damage progression under OP TMF and IP TMF [*1–7*] clearly shows that the former is controlled by matrix fatigue and the latter is controlled by a progression of fiber failures. Under IF, a change in mechanisms from matrix fatigue to fiber-dominated failure is observed with an increase in maximum applied stress [*8–11*]. Two-term models that account for both matrix fatigue and fiber-dominated failure have been proposed as a method to consolidate data of different cycle types and account for the difference in observed damage mechanisms [*1,12*]. Since life is controlled by the local behavior, damage parameters and tools used for monolithics can be used to describe the degradation in each constituent. In addition, time-dependent and environmental effects may also affect fatigue life. The final failure involves the failure of both fibers and matrix, but for a given test condition one of the constituents generally controls the damage progression during the majority of life.

Two analyses are conducted to predict the life: (1) the constituent response is determined using micromechanics, and (2) the cycles to failure is determined using a parameter or expression that is dependent on the constituent response and environmental conditions, including temperature and time. This investigation focuses primarily on the second item by examining a number of single correlating parameters based on either the fiber or matrix behavior and two models consisting of two terms. For all cases the constituent response is calculated using the same micromechanics model to make the comparisons among the different parameters and life models consistent.

Experiments

The experimental data include OP TMF, IP TMF, and IF tests conducted on unnotched SCS-6/Timetal 21S $[0]_4$ composite under load control in laboratory air atmosphere with the load applied parallel to the fibers. The stress ratio ($R = 0.1$) and number of plies were constant for all tests. However, the fiber volume fraction (V_f) varied among the specimens and is accounted for in the micromechanics modeling. The baseline TMF tests were con-

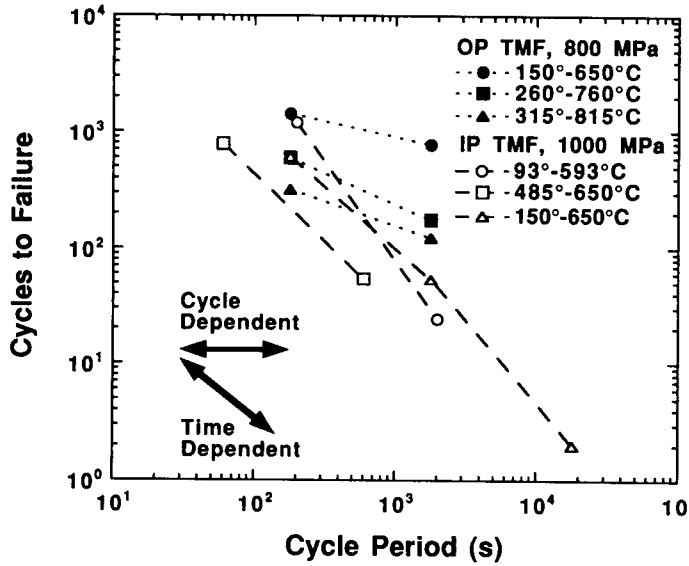

FIG. 1—*Effect of cycle period on OP and IP TMF life.*

ducted from 150 to 650°C at a frequency of 0.00556 Hz, and the baseline IF tests were conducted at 650°C at a similar frequency, 0.01 Hz. Cycles to failure is defined as the cycle when complete separation of the specimen occurs. The baseline data along with the details of the experiments are from Ref *6*. Further tests were then conducted to study how T_{max}, ΔT, and frequency affect the life compared to the baseline. Some of these results are summarized in Fig. 1. Increasing the cycle period (i.e., decreasing the frequency) decreases the life under both TMF phasings. However, the decrease under OP TMF ranges from a factor of 2 to 4, whereas the decrease under IP TMF is greater than a factor of 10. Thus OP TMF is both cycle and time dependent, whereas IP TMF is primarily time dependent. Additionally, under OP TMF an increase in T_{max} results in a decrease in life. Most of the OP TMF and IF data are reported in Ref *13*, although some of the IP TMF data are reported herein for the first time. All the experimental data are summarized in Tables 1 to 3.

Constituent Response

A 1-D micromechanics model (i.e., a rule of mixtures) with elastic fiber and viscoplastic matrix was used to determine the fiber and matrix response. Since this study involves tests conducted at different elevated temperatures and different frequencies, it is imperative that the micromechanics model accurately represents the time dependency of the composite behavior. To accomplish this, the matrix model was represented using the Bodner-Partom model [*14*] with constants given for Timetal 21S in Ref *15*. A good viscoplasticity model which represents the strain rate sensitivity of the matrix has been found to be more critical for obtaining the accurate axial response than a more complex geometric description [*16*].

TABLE 1—*Out-of-phase TMF tests.*

	Test Conditions					Computed Constituent Response					
Specimen ID	S_{max}, MPa	T_{min}, °C	T_{max}, °C	Frequency, Hz	V_f	σ^f_{max}, MPa	$\Delta\sigma^f$, MPa	σ^m_{max}, MPa	$\Delta\sigma^m$, MPa	$\Delta\epsilon^m$	N_f
Baseline											
92-179	1100	150	650	5.56E-03	0.32	1664	1503	835	750	0.00662	675
92-178	1000	150	650	5.56E-03	0.32	1455	1326	786	701	0.00617	919
92-177	900	150	650	5.56E-03	0.32	1246	1150	737	651	0.00572	1162
92-176	800	150	650	5.56E-03	0.32	1039	973	687	602	0.00527	1414
92-064	1100	150	650	5.56E-03	0.38	1572	1422	811	727	0.00641	911
92-065	900	150	650	5.56E-03	0.38	1193	1096	721	636	0.00558	1597
92-059	700	150	650	5.56E-03	0.37	820	775	630	546	0.00476	2112
92-060	600	150	650	5.56E-03	0.37	630	611	582	499	0.00434	3574
Others											
92-400	1000	150	815	4.18E-03	0.38	1520	1207	681	712	0.00704	198
92-398	800	150	815	4.18E-03	0.38	1118	868	605	630	0.00618	226
92-399	600	150	815	4.18E-03	0.38	708	524	534	550	0.00531	379
92-401	400	150	815	4.18E-03	0.38	302	180	460	470	0.00443	558
92-407	800	315	815	5.56E-03	0.38	1253	990	523	555	0.00582	316
92-408	800	260	760	5.56E-03	0.37	1201	952	565	584	0.00556	593
92-406	800	205	705	5.56E-03	0.38	1101	935	615	590	0.00535	1194
92-405	800	93	593	5.00E-03	0.38	944	945	712	582	0.00500	3573
92-410	800	650	815	1.67E-02	0.38	1751	1442	217	281	0.00510	732
92-411	800	485	650	1.67E-02	0.38	1386	1212	441	423	0.00431	4402
92-412	800	315	815	5.56E-04	0.38	1285	1037	503	532	0.00595	122
92-413	800	260	760	5.56E-04	0.38	1221	960	542	573	0.00558	175
93-118	800	150	650	5.56E-04	0.33	1092	976	656	595	0.00527	774

TABLE 2—*In-phase TMF tests.*

Specimen ID	Test Conditions					Computed Constituent Response					
	S_{max}, MPa	T_{min}, °C	T_{max}, °C	Frequency, Hz	V_f	σ^f_{max}, MPa	$\Delta\sigma^f$, MPa	σ^m_{max}, MPa	$\Delta\sigma^m$, MPa	$\Delta\epsilon^m$	N_f
Baseline											
92-173	900	150	650	5.56E-03	0.32	2496	2001	149	255	0.00270	229
92-172	800	150	650	5.56E-03	0.32	2186	1830	148	203	0.00222	1 097
92-175	700	150	650	5.56E-03	0.32	1877	1659	146	151	0.00175	6 251[a]
92-063	1100	150	650	5.56E-03	0.38	2656	2132	147	296	0.00306	208
92-061	1000	150	650	5.56E-03	0.38	2394	1973	146	248	0.00262	805
92-062	850	150	650	5.56E-03	0.38	2002	1735	144	175	0.00196	10 024[a]
Others											
93-115	1000	150	650	5.56E-03	0.34	2660	2100	145	287	0.00298	609
93-119	1000	93	593	5.00E-03	0.33	2408	2155	307	290	0.00325	1 189
93-116	1000	150	650	5.56E-04	0.34	2755	2077	96	296	0.00293	53
93-120	1000	93	593	5.00E-04	0.33	2650	2112	188	308	0.00317	24
93-122	1000	150	650	5.56E-05	0.33	2873	2100	78	310	0.00301	2
93-117	1000	485	650	1.67E-02	0.34	2626	1919	162	381	0.00413	780
93-121	1000	485	650	1.68E-03	0.33	2821	1932	103	394	0.00417	54

[a]Test was stopped before failure.

TABLE 3—*Isothermal fatigue tests.*

Specimen ID	Test Conditions				Computed Constituent Response					
	S_{max}, MPa	T, °C	Frequency, Hz	V_f	σ^f_{max}, MPa	$\Delta\sigma^f$, MPa	σ^m_{max}, MPa	$\Delta\sigma^m$, MPa	$\Delta\epsilon^m$	N_f
Baseline										
92-358	1000	650	1.00E − 02	0.37	2385	1797	187	373	0.00486	1 848
92-360	900	650	1.00E − 02	0.37	2145	1614	169	338	0.00436	2 343
92-357	800	650	1.00E − 02	0.37	1904	1432	152	302	0.00387	5 177
92-359	700	650	1.00E − 02	0.37	1659	1250	137	267	0.00338	9 990
Others										
92-208	1000	650	1.00E + 00	0.34	2274	1823	344	427	0.00493	3 722
92-204	900	650	1.00E + 00	0.35	1937	1616	342	379	0.00437	8 630
92-206	800	650	1.00E + 00	0.34	1694	1459	339	342	0.00394	25 749
92-168	700	650	1.00E + 00	0.35	1388	1257	330	295	0.00340	44 919
92-210	600	650	1.00E + 00	0.34	1157	1093	313	256	0.00296	87 910
92-205	600	650	1.00E + 00	0.34	1157	1093	313	256	0.00296	94 584
92-217	500	650	1.00E + 00	0.34	919	911	284	213	0.00246	729 019
92-207	800	815	1.00E + 00	0.34	2147	1706	106	212	0.00470	329
92-169	675	815	1.00E + 00	0.34	1798	1412	97	193	0.00389	7 412
92-209	550	815	1.00E + 00	0.34	1454	1131	84	168	0.00311	17 889
92-167	550	815	1.00E + 00	0.34	1454	1131	84	168	0.00311	20 663
92-171	450	815	1.00E + 00	0.34	1176	910	76	146	0.00251	53 196

The actual fiber volume fraction (V_f) for each experiment was used. A comparison between the 1-D model with a concentric cylinder model indicated that the average axial stress and strain values were similar when the composite was under an applied mechanical loading and varied by at most 15% when under a thermal loading only (i.e., when the applied stress was zero) [*17*]. Furthermore, the 1-D model ran about a factor of 10 faster than the concentric cylinder model. Since life prediction modeling tends to be highly empirical, small differ-

ences in the computed stress-strain response do not introduce inaccuracies in the life prediction as long as the same micromechanics model is used for all prediction analyses.

When a viscoplastic model is used, the constituent response is not initially stable and tends to ratchet toward some stabilized value. The ratchetting is caused by the stress relaxation of the matrix with the attendant increase in the fiber stress. Since the majority of the fatigue cycles occur under these stable conditions, the constituent response after stabilization is used in the prediction models. This is similar to using the strain or stress response at half life in low-cycle fatigue life prediction analyses. Similarly, Mirdamadi and Johnson ran VISCOPLY on a number of mission cycles until the response was stable [*4,18*].

The analysis of each test condition included a cooldown from 815°C that gives the thermal residual stresses, a ramp to the initial stress and temperature of the cycle, and ten thermal and mechanical cycles. A comparison of the model and experimental behavior at two frequencies under an IP TMF loading are given in Figs. 2 and 3. The model captures the inelastic strain on the first cycle as well as the ratchetting behavior with cycling. Since the model captures the composite behavior well, it provides confidence that the constituent behavior, which cannot be determined experimentally in the case of TMF, is also predicted well. The response of the constituents during processing and cycling for the two IP TMF cases are shown in Fig. 4. During the first nine cycles under IP TMF, the matrix stress relaxes, resulting in a 400-MPa increase in the fiber stress. The amount of increase in fiber stress is dependent on frequency, and for these two tests, the fiber stress is 250 MPa higher after nine cycles of a 30-min cycle compared to a 3-min cycle. In contrast, under OP TMF, the matrix relaxes very little and the response is nearly stable after the first cycle [*17,19*]. For OP TMF the maximum applied stress is at the low temperature of the cycle when the matrix is capable of carrying a greater portion of the load; consequently, the fiber stress is much lower under OP TMF. For illustration, the maximum fiber stresses at Cycle 10 under both IP and OP TMF with $V_f = 0.30$ and $T = 150$ to 650°C are shown in Fig. 5. The fiber stress under IP TMF is about twice as large. For this particular V_f, T_{max}, and ΔT, the increase in maximum fiber stress between a 3 and 30-min cycle is 150 MPa for IP TMF, whereas the frequency effect on fiber stress for OP TMF is somewhat less and decreases with decreasing maximum applied stress. The maximum fiber stress appears to be linearly related to the maximum stress applied to the composite. More details on the TMF response are given in Refs *17* and *19*. Since the constituent response is nearly stable after ten cycles, the response at Cycle 10 for each test condition is used in the life models. The response for each test is given in Tables 1 through 3.

Life Prediction Approaches

In this section a number of approaches are examined. First, approaches based solely on either the fiber response or matrix response are considered. However, these methods have limitations in predicting the general TMF response for many different stress-temperature-time histories. Two additional TMF models, the linear life fraction model (LLFM) and the dominant damage model (DDM), are considered that combine the effects of the fiber and matrix response to improve the TMF predictions over a wider range of test conditions. The DDM further incorporates environmental effects that help predict the T_{max}, ΔT, and frequency effects under TMF that are attributable to environment.

Based on Fiber Response

A number of researchers [*10,20–22*] have argued that since the fibers must fail to obtain composite failure, life is controlled by the fiber behavior. Therefore, the first parameter

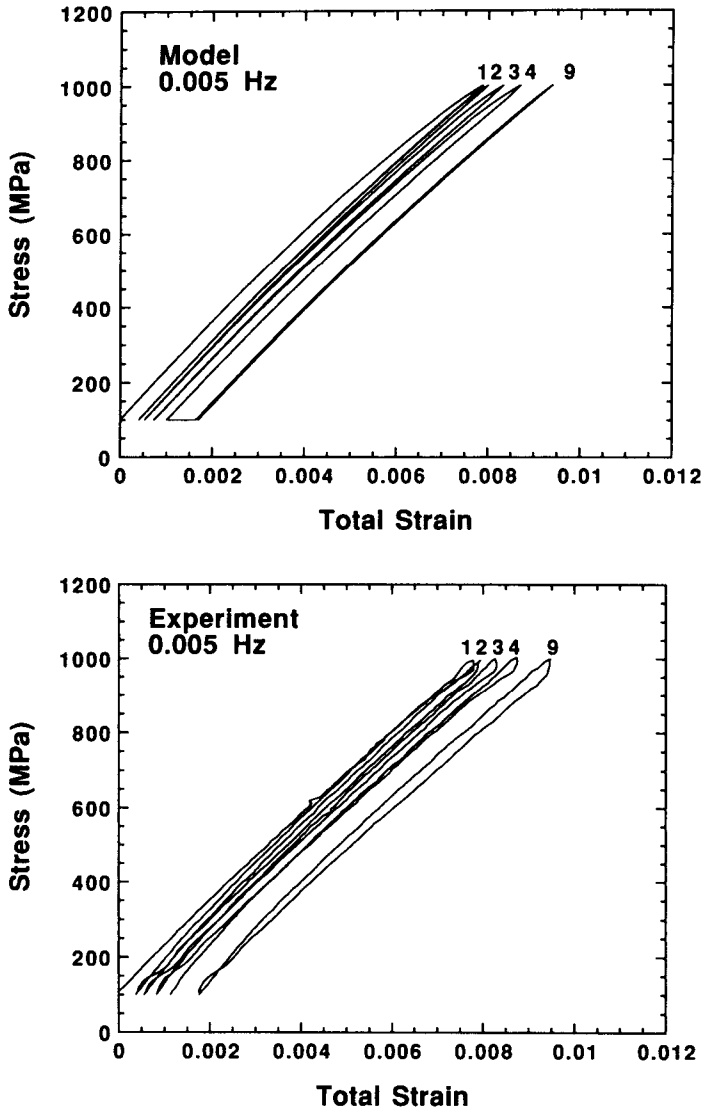

FIG. 2—*IP TMF response undergoing temperature cycle of 93 to 593°C at a frequency of 0.005 Hz* (V_f = *0.33):* (top) *model,* (bottom) *experiment.*

examined as a possible correlating parameter is the maximum fiber stress, σ^f_{max} (Fig. 6). The test data are separated by cycle types. The specific test conditions for each data point are given in Tables 1 through 3. The different cycle types tend to group together, with IP TMF and IF somewhat following a trend. For these tests an *S-N* curve for the fibers has been proposed [*21,23*]. Using σ^f_{max} assumes the strength of the fibers are degrading with number of cycles. In general, though, σ^f_{max} does not correlate all the data. If we say that σ^f_{max} correlates the IP TMF and IF data, the predictions for the OP TMF data are nonconservative

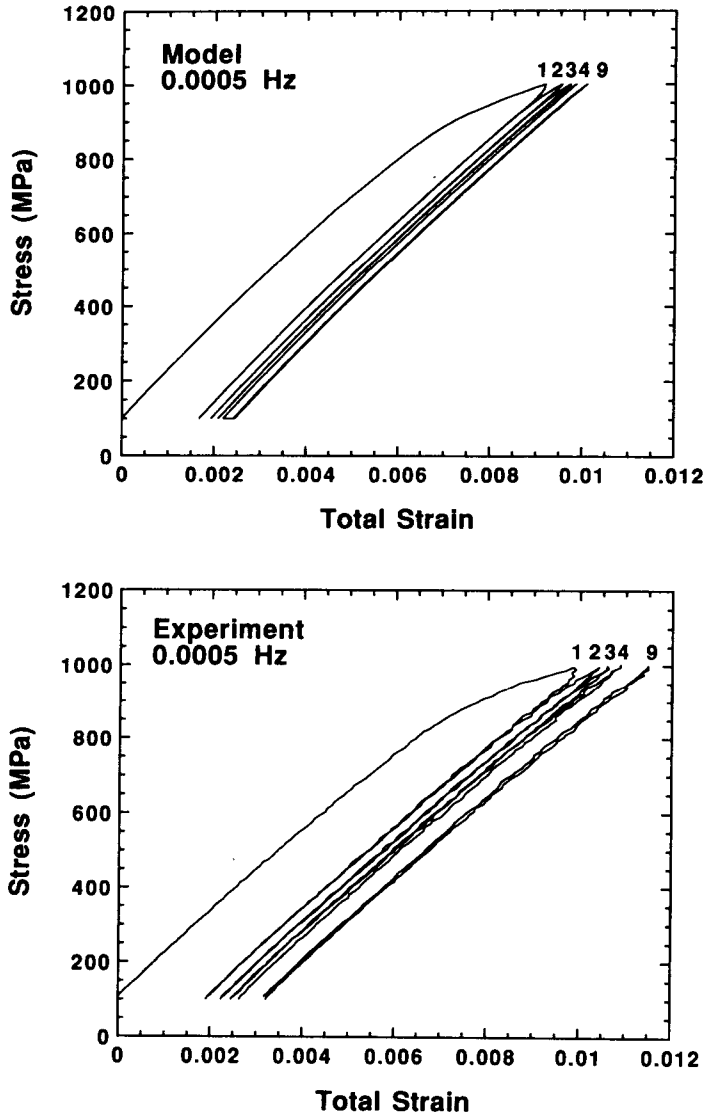

FIG. 3—*IP TMF response undergoing temperature cycle of 93 to 593°C at a frequency of 0.0005 Hz* ($V_f = 0.33$): (top) *model,* (bottom) *experiment.*

and the error is more than a factor of 10. The plot of σ^f_{max} is similar to plotting ϵ_{max} of the composite at the computed stabilized value because fiber and matrix are both subjected to the same strain while the stresses vary depending on the V_f and modulus of the constituents. The fiber response is elastic, though the modulus varies a small amount with temperature [*24*]. No fiber fracture is assumed to occur before the stabilized (Cycle 10) behavior is reached. So simply using ϵ_{max} of the stabilized composite response does not correlate the data any better.

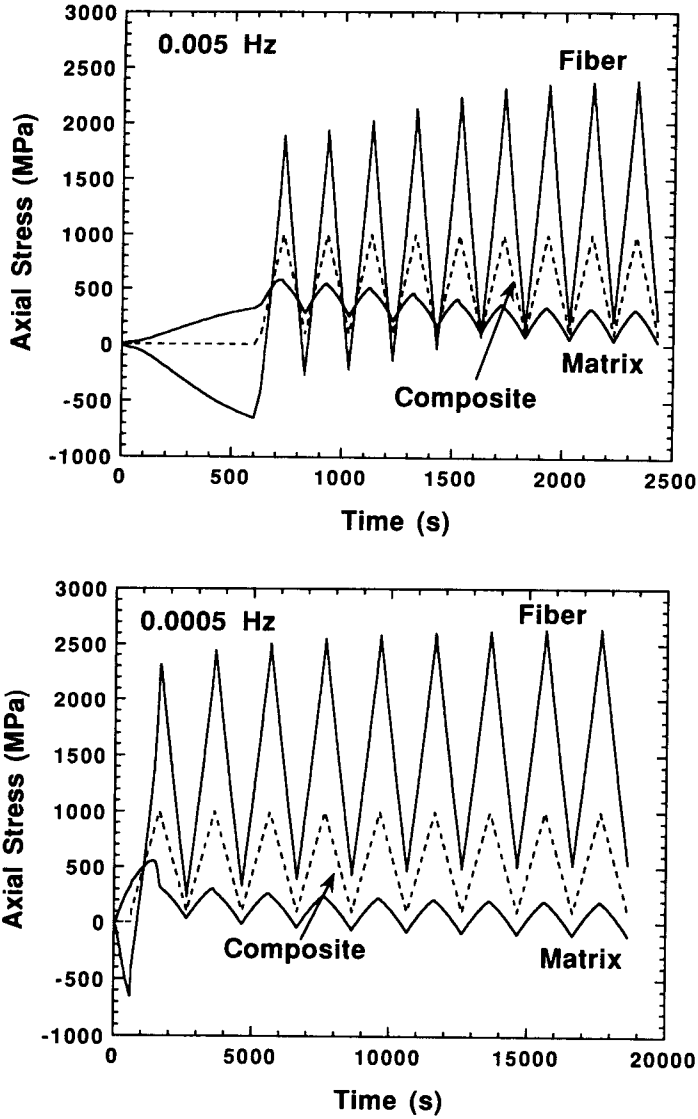

FIG. 4—*Fiber and matrix response for IP TMF undergoing temperature cycle of 93 to 593°C:* (top) *frequency of 0.005 Hz,* (bottom) *frequency of 0.0005 Hz.*

Others [*2,4,10,20*] have shown that fiber stress range ($\Delta\sigma^f$) can correlate the isothermal fatigue of different layups [*10,20*] as well as OP and IP TMF [*2,4*]. The fiber stress range has been successful in correlating tests of the same cycle type, but in general does not correlate different cycle types or variations in temperature and frequency [*4,25*]. Since $\Delta\sigma^f$ depends only on the range, it can be determined experimentally for isothermal fatigue by multiplying the composite strain range by the fiber modulus, eliminating the need to determine the thermal residual stress. For consistency though, the constituent behavior for

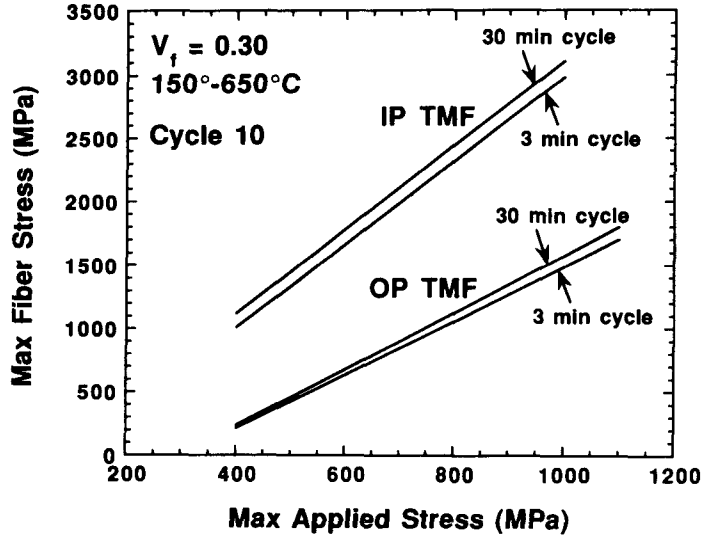

FIG. 5—*Computed maximum fiber stress for OP and IP TMF at cycle ten.*

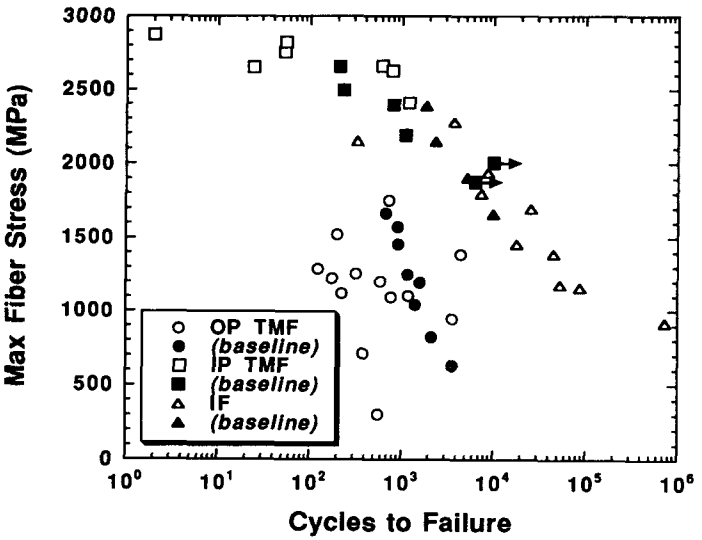

FIG. 6—*Correlation of all data based on maximum fiber stress.*

all cases was determined from the model. Plotting $\Delta\sigma^f$ seems to correlate all the data marginally better (Fig. 7), yet most of the OP TMF data still lie more than a factor of 10 away from IF and IP TMF data.

Recently Mirdamadi and Johnson [*18*] used $\sqrt{\Delta\sigma^f\sigma^f_{max}}$ as a correlating parameter and found it to work slightly better for their data. This parameter is motivated by the SWT parameter [*26*], which in this case accounts for both the cyclic effect as well as the mean stress effect on fiber degradation. However, no improvements in the correlation are realized for our data (Fig. 8). Mall et al. [*27*] introduced a term $\sigma^f_{max}(1 - R^f)^m$, $0 < m < 1$, to